Hindawi Publishing Corporation
Journal of Nanotechnology
Volume 2013, Article ID 768724, 8 pages
http://dx.doi.org/10.1155/2013/768724

Research Article

Amino-Functionalized Silica Nanoparticles: In Vitro Evaluation for Targeted Delivery and Therapy of Pancreatic Cancer

Abbey Y. Kardys, Dhruba J. Bharali, and Shaker A. Mousa

Pharmaceutical Research Institute at Albany College of Pharmacy and Health Sciences, 1 Discovery Drive, Rensselaer, NY 12144, USA

Correspondence should be addressed to Shaker A. Mousa; shaker.mousa@acphs.edu

Received 14 August 2012; Accepted 5 December 2012

Academic Editor: Thomas Thundat

We report a method of synthesis and optimization of amino-functionalized silica nanoparticles (SiNPs) and their in vitro evaluation as targeted delivery vehicles for the potential treatment of pancreatic cancer. SiNPs can efficiently encapsulate doxorubicin and can be attached to a targeting moiety such as anti-Claudin-4 (CLN4). The preferential uptake in pancreatic cancer cells, where CLN4 is overexpressed, of SiNPs when conjugated to CLN4 antibody (compared to nonconjugated SiNPs) was confirmed by confocal microscopy. SiNPs encapsulating doxorubicin had greater efficacy in MTT assays than free doxorubicin, and when conjugated to CLN4, the efficacy was dramatically increased (at 1 μM). No apparent carrier toxicity was observed when void SiNPs were used. SiNPs carrying a chemotherapeutic drug have the potential to be used as a targeted therapy for lethal cancers, such as pancreatic cancer. Also, incorporation of fluorescent probes in these SiNPs creates the possibility of their use as an imaging probe for diagnostic purposes.

1. Introduction

Cancer is still one of the most lethal diseases and one of the leading causes of death worldwide. Although there have been significant improvements in treating many cancers including breast, prostate, and lung with advances in medical technology, improvements in pancreatic cancer treatment have lagged behind. In the United States, pancreatic cancer is the fourth leading cause of cancer-related death. Aggressive disease progression and difficulties in early detection (before it metastasizes) are the two major factors that contribute to the ~95% death rate for patients suffering from pancreatic cancer. In most cancer treatments, the key to success relies mainly on early diagnosis, but in the case of pancreatic cancer currently available diagnosis technology is largely ineffective until the cancer progresses to late stages [1]. According to the American Association for Cancer Research, in 2012 there were an estimated 43,920 new cases of pancreatic cancer expected to occur, with 37,390 deaths [1]. Conventional treatment, which relies mainly on highly invasive chemotherapy, radiation, and surgery, has failed to impact the pancreatic cancer death rate because pancreatic cancer is resistant to most of the currently available chemo- and radiation therapies, and surgical removal of the primary tumor is fruitless owing to its high tendency to metastasize to distant organs. This is particularly true for individuals known to be "at risk" for developing pancreatic cancer because they have an inherited predisposition to it [2–5]. Therefore, the development of new alternative modalities and technologies is urgently needed in order to diagnose and treat pancreatic cancer at an early and hence potentially curative stage.

In the last 10 years, nanotechnology has profoundly impacted various fields of contemporary medicine [6–8], and its use has provided unprecedented opportunities to tackle many of the challenges in cancer treatment [9–12]. Nanotechnology has the potential to be used as an effective alternative in diagnosing and treating pancreatic cancer. Conventional cancer chemotherapy drugs are hampered by many problems including poor solubility and toxic side effects [13–15]. Nanoparticle-mediated drug delivery has the ability to reduce the unwanted toxic side effects by masking the drug via nanoparticle encapsulation and thus has the

potential to prevent adverse effects in normal cells. Another distinguishing feature of nanoparticle-mediated drug delivery is its potential use for targeted delivery to the cancer cells, thus significantly increasing the drug's availability to the tumor. Via targeted delivery of the chemotherapeutic load, a nanoparticle carrier system allows efficient and noninvasive treatment and may eliminate the need for invasive surgery and radiation therapy.

In last two decades, silica nanoparticles (SiNPs) have become a well-accepted choice for drug and gene therapy due to their safe history, good biocompatibility and biodegradability, and easily "tunable" surface functionality [16–18]. They have been used extensively for various applications including photothermal therapy [19], photodynamic therapy [20, 21], magnetic resonance imaging [22], peptide delivery [23], and gene delivery [24, 25]. SiNPs are "tunable" because they are easily modified with functional groups like –COOH and $–NH_2$, which allows conjugation with a target moiety for targeted delivery and, therefore, promotes better therapies as well as prognosis [26, 27]. Additionally, the use of SiNPs for drug delivery eliminates the use of toxic organic solvents in drug formulations because SiNPs can be dispersed in water and can help to increase the half-life of the encapsulated drug by sustained release.

Thus, considering their tremendous potential, we hypothesized that SiNPs might have the ability to provide an alternative method to address many of the challenges associated with conventional pancreatic cancer diagnosis and therapy. In particular, amino-functionalized SiNPs can be used to target to specific cell types by conjugating a cell-line-specific ligand or antibody in a relatively easy way. SiNPs will also enable us either to incorporate an anticancer drug or a fluorescent dye, or both, for more sensitive and effective imaging as well as therapies. In this study, we report the synthesis of amino-functionalized SiNPs encapsulating doxorubicin. These nanoparticles also can be labeled with Alexa Fluor 488 and conjugated to Claudin-4 antibody (CLN4), an antibody known to be specific to pancreatic cancer, and we describe the superior anticancer activity of doxorubicin-conjugated SiNPs conjugated to CLN4.

2. Materials and Methods

2.1. Materials. Ethanol, tetraethyl orthosilicate (TEOS), ammonium hydroxide, 3-aminopropyl triethoxysilane (APTES), doxorubicin, and formaldehyde were purchased from Sigma-Aldrich (St. Louis, MO, USA). Dulbecco's modified eagle medium (DMEM), phosphate buffered saline (PBS), fetal bovine serum (FBS), mouse anti-Claudin-4, and Alexa Fluor 488 N-hydroxysuccinimide dye were purchased from Invitrogen (Grand Island, NY, USA). 1-Ethyl-3-(3-dimethylaminopropyl)carbodiimide hydrochloride (EDC) was obtained from Polysciences, Inc. (Warrington, PA, USA). The human pancreatic carcinoma cell line Panc-1 was obtained from American Type Culture Collection (ATCC, Manassas, VA, USA).

2.2. Nanoparticles Synthesis. Amino-functionalized SiNPs were synthesized by synchronized hydrolysis of tetraethyl orthosilicate (TEOS) and 3-aminopropyl triethoxysilane (APTES) in the presence of ammonium hydroxide and ethanol by a method modified from Stöber [28–30]. In a typical experiment, 500 μL of TEOS, 500 μL of ammonium hydroxide, and 5 μL of APTES were added to 5 mL of ethanol and stirred for 2 hours using a magnetic stirrer. The solution was then dialyzed (10–12 kDa cutoff membrane) against DI water for 24 hours to remove unreacted materials. Similarly, SiNPs labeled with Alexa Fluor 488 were prepared by following the same procedure with the addition of 10 μL of Alexa Fluor 488 N-hydroxysuccinimide (1 mg/mL DMSO) to the 5 mL nanoparticles solution.

To prepare doxorubicin-encapsulated SiNPs, 10 μL doxorubicin (20 mg/mL DMSO) were added to 250 μL TEOS and 2.5 mL ethanol and stirred for 1 hour. Then, 250 μL ammonium hydroxide and 1 μL APTES were added and stirred for 2 hours. The solution was diluted to 6 mL total volume with DI water, then dialyzed (10–12 kDa cutoff membrane) against DI water for 24 hours to remove unreacted materials. The nanoparticles were lyophilized and redispersed in DI water for further use.

Anti-Claudin-4 (CLN4) was conjugated to the SiNPs using 1-ethyl-3-(3-dimethylaminopropyl)carbodiimide hydrochloride (EDC). Ten μL of EDC (10 mg/mL DI water), 5 μL of CLN4 (100 μg/200 μL DI water), and 1 mL DI water were stirred for 1 hour using a magnetic stirrer. Then, 1.5 mL of a solution of the lyophilized powder of the doxorubicin-encapsulated SiNPs dispersed in 10 mL of DI water was added and stirred for 4 hours using a magnetic stirrer. The solution was then dialyzed (10–12 kDa cutoff membrane) against DI water for 24 hours. Then the solution was frozen at −80°C, lyophilized for 24 hours, and redispersed in DI water.

2.3. Size, Zeta Potential, and Morphology. Nanoparticle size and zeta potential were measured using a Zetasizer Nano ZS (Malvern Instruments, Southborough, MA, USA). One mL of the SiNPs solution was added to a 1.5 mL plastic cuvette and measured using dynamic light scattering at 25°C. The size and morphology of the SiNPs were examined using a JEOL JEM-100CX transmission electron microscope (JEOL, Inc., Peabody, MA, USA). One drop of nanoparticles redispersed in DI water after lyophilization was mounted on a thin film of amorphous carbon deposited on a copper grid (300 meshes). It was then dried under clean conditions and the grid was examined directly with the transmission electron microscope.

2.4. Entrapment Efficiency. Entrapment efficiency of the doxorubicin was determined by filtering a known amount of SiNPs through a 100 kDa filter membrane to separate the free doxorubicin before dialysis. The amount of doxorubicin was determined using a Nanodrop UV spectrophotometer (Thermo Scientific, Wilmington, DE, USA). The entrapment efficiency (E%) was calculated using the value for the total concentration of doxorubicin (free + encapsulated) in the

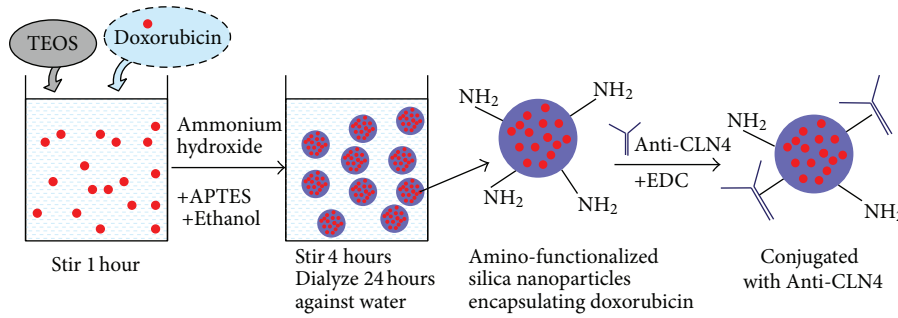

FIGURE 1: Schematic diagram showing the synthesis of amino-functionalized SiNPs encapsulating doxorubicin conjugated with anti-Claudin-4. Anti-CLN4: anti-Claudin-4; APTES: 3-aminopropyl triethoxysilane; EDC: 1-ethyl-3-(3-dimethylaminopropyl)carbodiimide hydrochloride; TEOS: tetraethyl ortho-silicate.

system, $[DOX]_0$, and that in the filtrate, $[DOX]_f$, using the equation:

$$E\% = \left(\frac{\left([DOX]_0 - [DOX]_f\right)}{[DOX]_0}\right) \times 100. \quad (1)$$

2.5. Release Kinetics of Doxorubicin from the Nanoparticles. A known amount of lyophilized SiNPs encapsulating doxorubicin was resuspended in 5 mL PBS and the solution was kept at room temperature. At predetermined time intervals, the solution was vortexed and a 400 μL aliquot was removed and filtered through a 100 kDa cutoff membrane filter by centrifugation at 6000 rpm to separate the released doxorubicin from the SiNPs. The concentration of the released doxorubicin at each time point was determined using the Nanodrop UV spectrophotometer. The percent release of doxorubicin at each time point was calculated by using the equation [31]:

$$\%\text{release} = \left(\frac{[DOX]_{f,t}}{[DOX]_0}\right) \times 100, \quad (2)$$

where $[DOX]_{f,t}$ is the concentration of doxorubicin in the filtrate at time t. Similarly, to study the release kinetics of doxorubicin in FBS, a known amount of lyophilized SiNPs encapsulating doxorubicin was suspended in 10 mL of 20% FBS. The release kinetics were studied exactly as described above for PBS.

2.6. Cell Culture and Confocal Imaging. A human pancreatic carcinoma cell line (Panc-1) was maintained in DMEM with 10% FBS, according to the manufacturer's instructions. The cells were trypsinized and resuspended in DMEM at a concentration of around 5×10^5 cells/mL. Sixty μL of this suspension were transferred to a 35 mm culture plate and 2 mL of full medium were added. The plates were then placed in an incubator (model 2400, VWR Scientific, Radnor, PA, USA) at 37°C with 5% CO_2. After 24 hours, the cells (70% confluency) were rinsed with PBS, and 2 mL of fresh media were added to the plates. Fifty μL of either CLN4-conjugated SiNPs or control SiNPs were added and mixed. For competitive binding experiments, plates were preincubated with 50 μL of anti-CLN4 for 4 hours and then 50 μL of CLN4-conjugated SiNPs were added. The plates were returned to the incubator (37°C, 5% CO_2). After 3 hours, the plates were taken out, rinsed several times with sterile PBS, and the cells were fixed with 1% formaldehyde. The plates were imaged directly under a confocal microscope (Leica TCS SP5, Exton, PA, USA). A 405 nm laser was used for excitation and the emission was detected between 510 nm and 550 nm.

2.7. MTT Assay. A human pancreatic carcinoma cell line (Panc-1) was maintained in DMEM with 10% FBS, according to the manufacturer's instructions. The cells were trypsinized and resuspended in DMEM at a concentration of around 1.55×10^5 cells/mL. One hundred μL of this suspension were added to each well of a 96-well plate. The plates were then placed in an incubator at 37°C with 5% CO_2 for 48 hours. Fifteen μL of either void SiNPs, doxorubicin-encapsulated SiNPs, doxorubicin-encapsulated SiNPs conjugated with CLN4, or free doxorubicin were added to each well in a column. After 48 hours of incubation, cell viability was estimated using a colorimetric MTT assay as per the protocol provided by the supplier (Invitrogen).

3. Results

3.1. Nanoparticles Synthesis. A schematic diagram showing the preparation of SiNPs encapsulating doxorubicin is shown in Figure 1. The nanoparticles can be attached to a dye through their free $-NH_2$ group owing to the presence of APTES. Depending on the amount of ethanol, APTES, and TEOS, the size and surface charge (zeta potential) of the nanoparticles can be manipulated.

3.2. Determination of Size, Zeta Potential, and Morphology. Diagrams showing the typical sizes of the nanoparticles are shown in Figures 2(a)–2(c). We have observed that depending on various parameters like the amount of TEOS, APTES, and ammonia, the size of the nanoparticles can be manipulated; a SiNP size anywhere between 35 nm and 500 nm can be obtained by this method. To see the effect of APTES, we synthesized nanoparticles only with TEOS in the absence of APTES. From Figure 2(d), it is clear that the

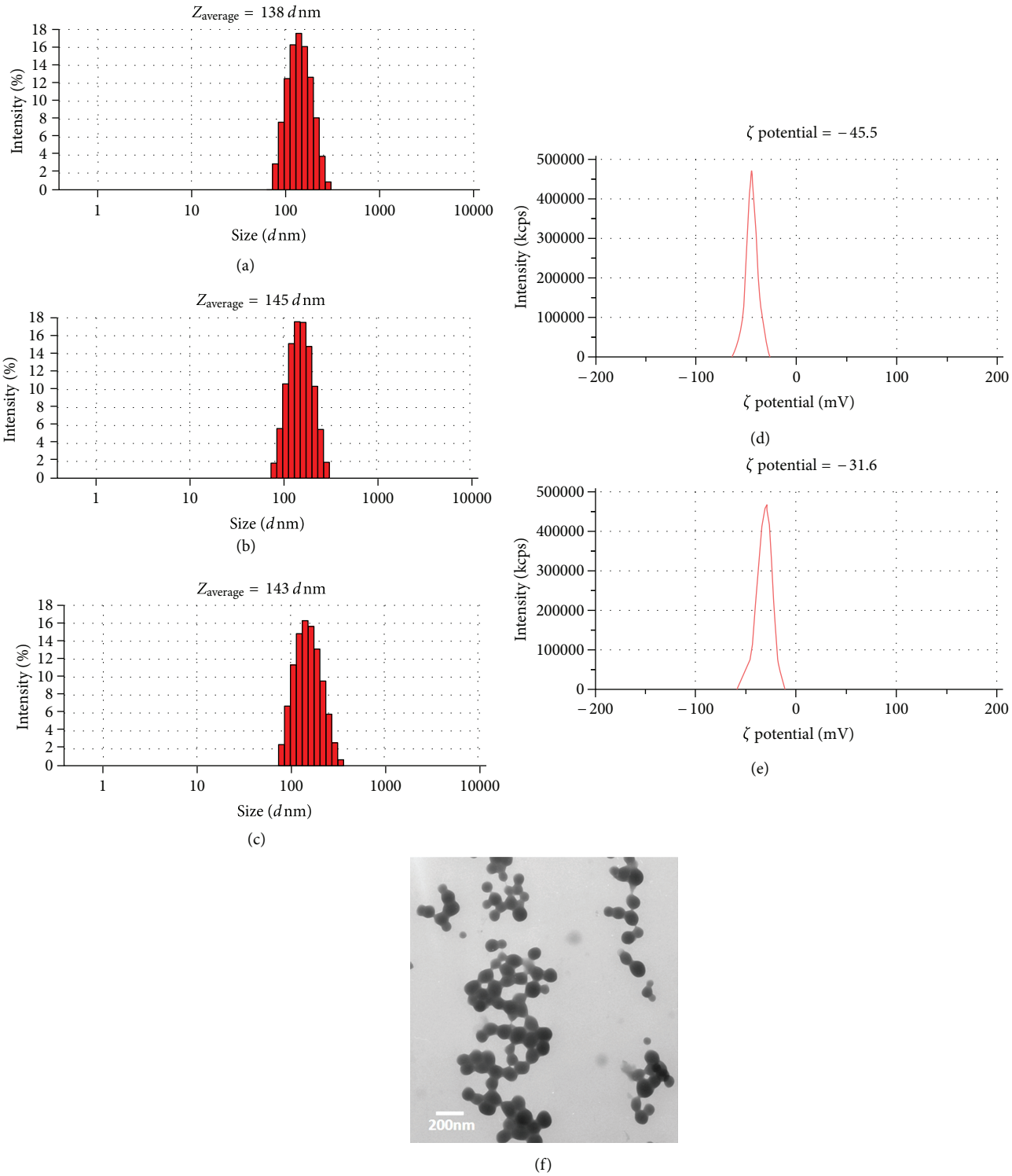

Figure 2: Size measurement by dynamic light scattering. (a) SiNPs that are not amino-functionalized (without APTES), (b) SiNPs that are amino-functionalized (with APTES), and (c) SiNPs-CLN4 (amino-functionalized nanoparticles conjugated to anti-Claudin-4). Measurement of zeta potential (surface charge) of (d) SiNPs (not amino-functionalized) and (e) SiNPs amino-functionalized. (f) Transmission electron microscope image showing the size and morphology of SiNPs encapsulating doxorubicin and conjugated to CLN4. d nm: diameter in nanometers.

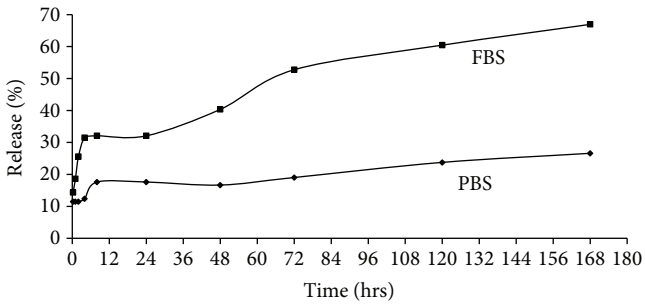

Figure 3: Release kinetics of doxorubicin from the SiNPs in phosphate buffered saline (PBS) and fetal bovine serum (FBS).

zeta potential of the nanoparticles was around −45 mV when there was no APTES, that is, in the absence of an $-NH_2$ group. But when synthesized with APTES, the zeta potential decreased to around −31 mV (Figure 2(e)). A transmission electron microscope image showing the size and morphology of SiNPs encapsulating doxorubicin and conjugated to CLN4 is shown in Figure 2(f).

3.3. Entrapment Efficiency. The entrapment efficiency of doxorubicin was found to be ~70%, and the loading efficiency of the nanoparticles was around 2% w/w of total weight of the nanoparticles.

3.4. Release Kinetics. To evaluate the pattern of release of doxorubicin from SiNPs, we studied the release kinetics in two physiological systems, PBS and 20% FBS, for 7 days. The cumulative percentage of doxorubicin released from the nanoparticles at different time intervals is shown in Figure 3. The percentage of released doxorubicin, shown at absolute zero time, is not truly zero time; there is always an inherent delay between the mixing of the nanoformulation and the separation of the released doxorubicin in both PBS and 20% FBS. In FBS, there was rapid release of doxorubicin (>30%) within the first 8 hours and then a steady but relatively slow release of doxorubicin. In PBS, the release was slow compared to that of FBS. Cumulatively, at the end of a one-week study, we found that around 70% of doxorubicin was released in FBS whereas there was only 25% release in PBS.

3.5. Confocal Imaging. The confocal images showing the uptake in Panc-1 cells of void SiNPs and CLN4-conjugated SiNPs labeled with Alexa Fluor 488 are shown in Figure 4. It is clear that after 3 hours of incubation, there was a significant increase in uptake of SiNPs when conjugated to CLN4 antibody (Figure 4(a)) compared to the SiNPs only (without CLN4, Figure 4(b)). There was no significant uptake of the SiNPs-CLN4 when the cells were preincubated for 4 hours with anti-CLN4 (data not shown). The increase of the fluorescent intensity was further confirmed by the confocal microscopy spectral intensity quantification (data not shown). This result is a proof of our hypothesis that there is specific uptake of nanoparticles when conjugated to an antibody specific to a tumor cell.

3.6. MTT Assays and In Vitro Efficacy Studies. Further evidence for the increased uptake of SiNPs conjugated to CLN4 was found in the MTT assay data, as shown in Figure 5. It is clear that at low concentrations (0.1 μM) of doxorubicin, either encapsulated in SiNPs or encapsulated in SiNPs conjugated to CLN4, SiNPs do not have significant cytotoxic effects in Panc-1 cells. At higher concentrations (10 μM) of doxorubicin, however, there was significant toxicity, but this activity appeared to be nonspecific. At a 1 μM concentration of doxorubicin, free doxorubicin does not exert a toxic effect on Panc-1 cells. However, when doxorubicin at a concentration of 1 μM is encapsulated in SiNPs, the toxicity increases significantly. Toxicity increases further when 1 μM doxorubicin-encapsulated SiNPs are conjugated with CLN4.

3.7. Nanoparticle Size Manipulation. The size of the nanoparticles can be manipulated by altering various parameters (Figure 6). By varying the amount of ammonium hydroxide (75 μL to 500 μL), we were able to get a size as small as ~35 nm to as big as 335 nm in diameter (Figure 6(a)). Ammonium hydroxide was used as a catalyst and is well known to increase the rate of hydrolysis. The size increase from 35 nm to 350 nm with the increase in ammonium hydroxide is because of the formation of a bulkier silica network due to increased hydrolysis. Ethanol serves as the reaction medium, so when the volume of ethanol is increased (Figure 6(b)) there is less chance for interaction between the reactants. The size of the SiNPs was also examined at various reaction time points to determine the effect of the reaction time on the size of the SiNPs and to obtain an optimum reaction time to get the required size (Figure 6(c)). There was a rapid increase in the nanoparticles' size in the initial reaction time period, and as reaction time increased the size became more uniform. The size remained more or less constant after 1 hour. Thus, a 1 hour reaction time is the optimum reaction time for this nanosynthesis.

4. Discussion

Our synthesis of amino-functionalized SiNPs by synchronized hydrolysis of TEOS and APTES in the presence of ethanol and ammonium hydroxide was based on modifying a method originally developed by Stöber [28]. The main advantage of this method is that the synthesis of nanoparticles can be performed in organic solvent and the resultant nanoparticles can be dispersed in aqueous medium. This method can be used primarily as a platform for various water-insoluble drugs, and, therefore, the use of toxic organic solvents and excipients is avoided. The SiNPs synthesized by this method can be controlled by various parameters and therefore gives us more flexibility as per as the need. Though we have tried to encapsulate doxorubicin in different-sized nanoparticles (data not shown), the maximum entrapment efficiency of doxorubicin was found to be around 70% with nanoparticles sized around 150 nm in diameter.

The surface charge of the nanoparticles was measured in order to see any difference due to the presence of the APTES, which has positively charged $-NH_2$ groups; the presence of an

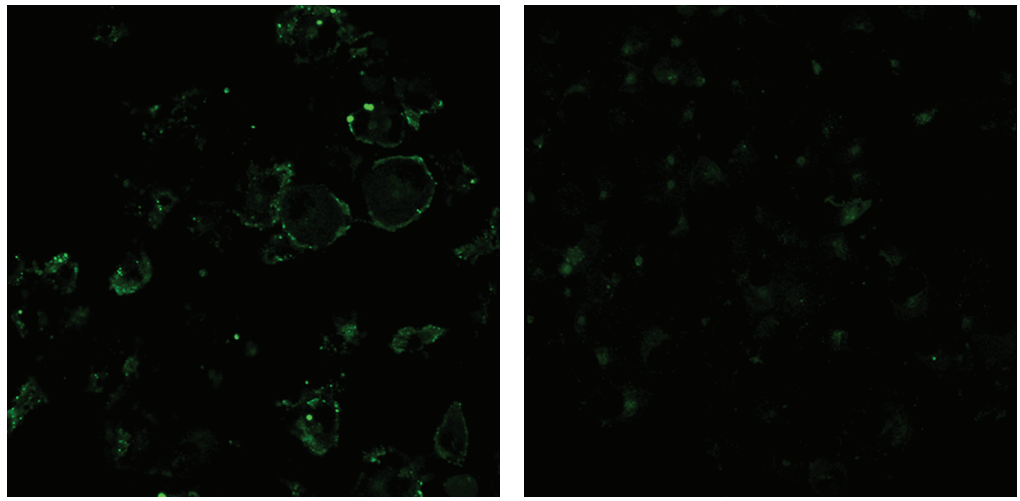

(a) (b)

Figure 4: Confocal images showing the uptake of SiNPs in Panc-1 cells after 3 hours of incubation. (a) SiNPs-Alexa Fluor 488-CLN4; (b) SiNPs-Alexa Fluor 488.

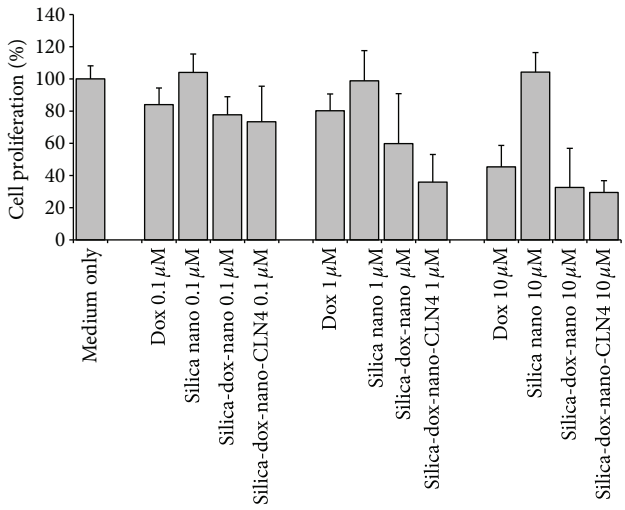

Figure 5: Panc-1 cell proliferation and cytotoxic effect on Panc-1 cells of different formulations. Void SiNPs and free doxorubicin were used as controls. Medium only means nontreated cells. Dox: doxorubicin.

amino group should increase the zeta potential because of its positive charge. Thus, as per our comparison, we prepared the same kind of nanoparticles without the presence of APTES, and, as anticipated, the zeta potential increased from −45 mV to −31 mV. This is also indirect evidence showing that the amino group is conjugated to the SiNPs, and that there is synchronized hydrolysis happening between the APTES and TEOS.

The entrapment efficiency of doxorubicin was found to be more than ~70%, indicating that the loss of doxorubicin during the synthesis was not significant. We predict that the high encapsulation efficiency of doxorubicin in the silica nanoparticles is because of charge interaction between silica and doxorubicin [32]. In the case of FBS, after the initial ~30% release within the first 4 hours, there was a steady, constant release of doxorubicin from the nanoformulation, with the observation of ~70% encapsulated doxorubicin released within one week. Thus, this "burst effect" for doxorubicin could be due to the presence of dissolved proteins, glucose, clotting factor, and so forth present in FBS. Additionally, the sustained release of doxorubicin in FBS (a system that mimics the human blood system) shows the potential effect these nanoparticles have as a nanoreservoir for doxorubicin, and thus may be able to eliminate multiple-injection dose regimens. The low release of doxorubicin in PBS is because of stronger ionic interactions of doxorubicin in physiological buffer [32].

In most pancreatic cell lines, including Panc-1, Claudin-4 is overexpressed [33–35]. To exploit this, we have conjugated CLN4 antibody to dye-labeled nanoparticles for specific delivery to Panc-1 cells. Thus, as hypothesized, the uptake of the nanoparticles significantly increased when they were conjugated to dye-labeled nanoparticles. Quantification of the fluorescent intensity in the cells by confocal microscopy (data not shown) also supports our hypothesis of targeted delivery. Since Claudin-4 is overexpressed in the Panc-1 cell line, SiNPs with the antibody can be taken up faster by receptor-mediated endocytosis compared to SiNPs without it, which can only be taken up by nonselective endocytosis. No significant uptake of the SiNPs-CLN4 in Panc-1 cells preincubated with anti-CLN4 is strong evidence that it was receptor-mediated uptake. The increased fluorescent intensity observed in the Panc-1 cells by confocal imaging further confirms that there was receptor-mediated uptake due to the presence of CLN4 antibody in the SiNPs. On the other hand, there was little fluorescence observed from the Panc-1 cells when the cells were incubated with void nanoparticles. This little uptake of the void silica nanoparticles into the cells may be due to nonspecific endocytosis.

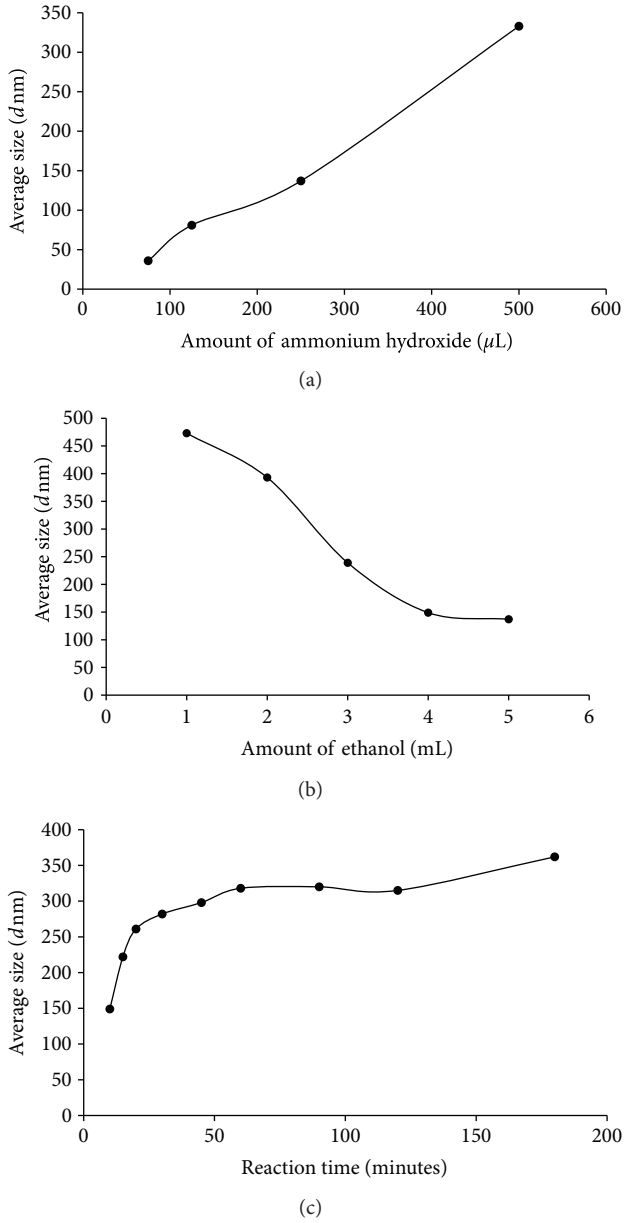

Figure 6: Effect on size of nanoparticles of (a) amount of ammonium hydroxide, (b) amount of ethanol, and (c) reaction time. d nm: diameter in nanometers

The potential of SiNPs as a delivery vehicle for targeted delivery to pancreatic cancer cells was further evidenced by delivering doxorubicin encapsulated into SiNPs with or without conjugating CLN4 antibody on the surface of the SiNPs. All the formulations, including free doxorubicin, were not effective at lower concentrations (0.1 μM). At higher concentrations, a higher cytotoxic effect was observed in all formulations; however, there was little difference between the different treatments. This may be because of the high concentration of doxorubicin, and may not be the optimum dose without harming the healthy cells when injected in vivo. We found that the optimum concentration for doxorubicin is a 1 μM solution. Since Claudin-4 antigen is overexpressed in Panc-1 cells, nanoparticles with CLN4 antibody have the capacity to increase the uptake of the SiNPs to this type of pancreatic cells. Alternatively, the doxorubicin uptake was increased because of the presence of Claudin-4 antibody on the surface of the SiNPs and thus the cytotoxicity of the formulation was enhanced. One of the most important observations during this experiment was that there was no apparent void SiNPs-related toxicity on the Panc-1 cells, and thus we can conclude from these preliminary in vitro results that SiNPs are a potentially safe vehicle and have the potential to be used for in vivo experiments for further studies.

5. Conclusions

We have synthesized amino-functionalized SiNPs encapsulating doxorubicin conjugated to CLN4 antibody with a relatively simple, one-step method. The size of the SiNPs was found to be dependent on the amounts of ethanol, ammonium hydroxide, and reaction time. Though we used SiNPs of ~150 nm in size, nanoparticles from 35 nm to 500 nm can be synthesized by manipulating various parameters. Confocal imaging showed that there was a higher uptake of CLN4-conjugated SiNPs in the Panc-1 cells compared to void SiNPs. CLN4-conjugated SiNPs encapsulating doxorubicin have a greater toxicity than free doxorubicin in the Panc-1 cell line. The results from our preliminary in vitro experiments in this study show that this tiny SiNP system has potential as a targeted delivery vehicle for pancreatic cancer. Though there is a need to perform in vivo studies to prove our hypothesis of targeting pancreatic cancer with a nanoparticle-mediated delivery system, we consider this current study might be a major breakthrough towards developing treatments for pancreatic cancer in the near future. Furthermore, the tunable surface functionality of this SiNPs system has the tremendous potential to allow attachment of other imaging modalities like an MRI/PET imaging probe instead of a fluorescent dye. These imaging modalities are widely used in clinical practices for cancer diagnosis. Thus, targeted delivery using SiNPs with an imaging probe might have the potential to be used as a sensitive probe to detect pancreatic cancer in an early stage, and hence in a potentially curative stage.

Conflict of Interests

The authors declare that they have no conflict of interests.

References

[1] American Cancer Society, *Cancer Facts & Figures 2012*, pp. 19, http://www.cancer.org/Research/CancerFactsFigures/CancerFactsFigures/cancer-facts-figures-2012.

[2] R. T. Greenlee, M. B. Hill-Harmon, T. Murray, and M. Thun, "Cancer statistics, 2001," *A Cancer Journal for Clinicians*, vol. 51, no. 1, pp. 15–36, 2001.

[3] T. P. Yeo, R. H. Hruban, S. D. Leach et al., "Pancreatic cancer," *Current Problems in Cancer*, vol. 26, no. 4, pp. 176–275, 2002.

[4] R. H. Hruban, G. M. Petersen, M. Goggins et al., "Familial pancreatic cancer," *Annals of Oncology*, vol. 10, supplement 4, pp. 69–73, 1999.

[5] G. M. Petersen and R. H. Hruban, "Familial pancreatic cancer: where are we in 2003?" *Journal of the National Cancer Institute*, vol. 95, no. 3, pp. 180–181, 2003.

[6] D. F. Emerich and C. G. Thanos, "Nanotechnology and medicine," *Expert Opinion on Biological Therapy*, vol. 3, no. 4, pp. 655–663, 2003.

[7] T. Kubik, K. Bogunia-Kubik, and M. Sugisaka, "Nanotechnology on duty in medical applications," *Current Pharmaceutical Biotechnology*, vol. 6, no. 1, pp. 17–33, 2005.

[8] S. E. Leucuta, "Nanotechnology for delivery of drugs and biomedical applications," *Current Clinical Pharmacology*, vol. 5, no. 4, pp. 257–280, 2010.

[9] D. J. Bharali and S. A. Mousa, "Emerging nanomedicines for early cancer detection and improved treatment: current perspective and future promise," *Pharmacology & Therapeutics*, vol. 128, no. 2, pp. 324–335, 2010.

[10] M. Ferrari, "Cancer nanotechnology: opportunities and challenges," *Nature Reviews Cancer*, vol. 5, no. 3, pp. 161–171, 2005.

[11] S. Nie, Y. Xing, G. J. Kim, and J. W. Simons, "Nanotechnology applications in cancer," *Annual Review of Biomedical Engineering*, vol. 9, pp. 257–288, 2007.

[12] S. Singhal, S. Nie, and M. D. Wang, "Nanotechnology applications in surgical oncology," *Annual Review of Medicine*, vol. 61, pp. 359–373, 2010.

[13] G. S. Kwon, "Polymeric micelles for delivery of poorly water-soluble compounds," *Critical Reviews in Therapeutic Drug Carrier Systems*, vol. 20, no. 5, pp. 357–403, 2003.

[14] C. M. Walko and H. McLeod, "Pharmacogenomic progress in individualized dosing of key drugs for cancer patients," *Nature Clinical Practice Oncology*, vol. 6, no. 3, pp. 153–162, 2009.

[15] I. Brigger, C. Dubernet, and P. Couvreur, "Nanoparticles in cancer therapy and diagnosis," *Advanced Drug Delivery Reviews*, vol. 54, no. 5, pp. 631–651, 2002.

[16] J. Lu, M. Liong, J. I. Zink, and F. Tamanoi, "Mesoporous silica nanoparticles as a delivery system for hydrophobic anticancer drugs," *Small*, vol. 3, no. 8, pp. 1341–1346, 2007.

[17] T. Y. Ohulchanskyy, I. Roy, L. N. Goswami et al., "Organically modified silica nanoparticles with covalently incorporated photosensitizer for photodynamic therapy of cancer," *Nano Letters*, vol. 7, no. 9, pp. 2835–2842, 2007.

[18] R. Kumar, I. Roy, T. Y. Ohulchanskyy et al., "Covalently dye-linked, surface-controlled, and bioconjugated organically modified silica nanoparticles as targeted probes for optical imaging," *ACS Nano*, vol. 2, no. 3, pp. 449–456, 2008.

[19] H. Yan, C. Teh, S. Sreejith, L. Zhu, A. Kwok, W. Fang et al., "Functional mesoporous silica nanoparticles for photothermal-controlled drug delivery in vivo," *Angewandte Chemie*, vol. 51, no. 33, pp. 8373–8377, 2012.

[20] M. Gary-Bobo, Y. Mir, C. Rouxel, D. Brevet, O. Hocine, M. Maynadier et al., "Multifunctionalized mesoporous silica nanoparticles for the in vitro treatment of retinoblastoma: drug delivery, one and two-photon photodynamic therapy," *International Journal of Pharmaceutics*, vol. 432, no. 1-2, pp. 99–104, 2012.

[21] I. Roy, T. Y. Ohulchanskyy, H. E. Pudavar et al., "Ceramic-based nanoparticles entrapping water-insoluble photosensitizing anticancer drugs: a novel drug-carrier system for photodynamic therapy," *Journal of the American Chemical Society*, vol. 125, no. 26, pp. 7860–7865, 2003.

[22] P. Sharma, N. E. Bengtsson, G. A. Walter, H. B. Sohn, G. Zhou, N. Iwakuma et al., "Gadolinium-doped silica nanoparticles encapsulating indocyanine green for near infrared and magnetic resonance imaging," *Small*, vol. 8, no. 18, pp. 2856–2868, 2012.

[23] P. Wang, X. Hu, S. Cook, and H. M. Hwang, "Influence of silica-derived nano-supporters on cellobiase after immobilization," *Applied Biochemistry and Biotechnology*, vol. 158, no. 1, pp. 88–96, 2009.

[24] D. J. Bharali, I. Klejbor, E. K. Stachowiak et al., "Organically modified silica nanoparticles: a nonviral vector for in vivo gene delivery and expression in the brain," *Proceedings of the National Academy of Sciences of the United States of America*, vol. 102, no. 32, pp. 11539–11544, 2005.

[25] D. Luo and W. M. Saltzman, "Enhancement of transfection by physical concentration of DNA at the cell surface," *Nature Biotechnology*, vol. 18, no. 8, pp. 893–895, 2000.

[26] W. Tan, K. Wang, X. He et al., "Bionanotechnology based on silica nanoparticles," *Medicinal Research Reviews*, vol. 24, no. 5, pp. 621–638, 2004.

[27] S. Santra, P. Zhang, K. Wang, R. Tapec, and W. Tan, "Conjugation of biomolecules with luminophore-doped silica nanoparticles for photostable biomarkers," *Analytical Chemistry*, vol. 73, no. 20, pp. 4988–4993, 2001.

[28] L. M. Rossi, L. Shi, F. H. Quina, and Z. Rosenzweig, "Stober synthesis of monodispersed luminescent silica nanoparticles for bioanalytical assays," *Langmuir*, vol. 21, no. 10, pp. 4277–4280, 2005.

[29] H. Flachsbart and W. Stöber, "Preparation of radioactively labeled monodisperse silica spheres of colloidal size," *Journal of Colloid and Interface Science*, vol. 30, no. 4, pp. 568–573, 1969.

[30] K. Stalder and W. Stober, "Haemolytic activity of suspensions of different silica modifications and inert dusts," *Nature*, vol. 207, no. 999, pp. 874–875, 1965.

[31] D. J. Bharali, V. Pradhan, G. Elkin et al., "Novel nanoparticles for the delivery of recombinant hepatitis B vaccine," *Nanomedicine*, vol. 4, no. 4, pp. 311–317, 2008.

[32] H. Meng, M. Liong, T. Xia et al., "Engineered design of mesoporous silica nanoparticles to deliver doxorubicin and P-glycoprotein siRNA to overcome drug resistance in a cancer cell line," *ACS Nano*, vol. 4, no. 8, pp. 4539–4550, 2010.

[33] P. Michl, M. Buchholz, M. Rolke et al., "Claudin-4: a new target for pancreatic cancer treatment using Clostridium perfringens enterotoxin," *Gastroenterology*, vol. 121, no. 3, pp. 678–684, 2001.

[34] C. A. Foss, J. J. Fox, G. Feldmann et al., "Radiolabeled anti-claudin 4 and anti-prostate stem cell antigen: initial imaging in experimental models of pancreatic cancer," *Molecular Imaging*, vol. 6, no. 2, pp. 131–139, 2007.

[35] H. Yamaguchi, T. Kojima, T. Ito, D. Kyuno, Y. Kimura, M. Imamura et al., "Effects of Clostridium perfringens enterotoxin via claudin-4 on normal human pancreatic duct epithelial cells and cancer cells," *Cellular & Molecular Biology Letters*, vol. 16, no. 3, pp. 385–397, 2011.